

## Charged Gold Nanoparticles with Essentially Zero Serum Protein Adsorption in Undiluted Fetal Bovine Serum

Avinash K. Murthy,<sup>†</sup> Robert J. Stover,<sup>‡</sup> William G. Hardin,<sup>‡</sup> Robert Schramm,<sup>†</sup> Golay D. Nie,<sup>†</sup> Sai Gourisankar,<sup>†</sup> Thomas M. Truskett,<sup>†</sup> Konstantin V. Sokolov,<sup>‡,§</sup> and Keith P. Johnston<sup>\*,†</sup>

<sup>†</sup>McKetta Department of Chemical Engineering, <sup>‡</sup>Department of Biomedical Engineering, and <sup>‡</sup>Texas Materials Institute, University of Texas at Austin, Austin, Texas 78712, United States

<sup>§</sup>Department of Imaging Physics, The University of Texas MD Anderson Cancer Center, Houston, Texas 77030, United States

### S Supporting Information

**ABSTRACT:** The adsorption of even a single serum protein molecule on a gold nanosphere used in biomedical imaging may increase the size too much for renal clearance. In this work, we designed charged  $\sim 5$  nm Au nanospheres coated with binary mixed-charge ligand monolayers that do not change in size upon incubation in pure fetal bovine serum (FBS). This lack of protein adsorption was unexpected in view of the fact that the Au surface was moderately charged. The mixed-charge monolayers were composed of anionic citrate ligands modified by place exchange with naturally occurring amino acids: either cationic lysine or zwitterionic cysteine ligands. The zwitterionic tips of either the lysine or cysteine ligands interact weakly with the proteins and furthermore increase the distance between the “buried” charges closer to the Au surface and the interacting sites on the protein surface. The  $\sim 5$  nm nanospheres were assembled into  $\sim 20$  nm diameter nanoclusters with strong near-IR absorbance (of interest in biomedical imaging and therapy) with a biodegradable polymer, PLA(1k)-*b*-PEG(10k)-*b*-PLA(1k). Upon biodegradation of the polymer in acidic solution, the nanoclusters dissociated into primary  $\sim 5$  nm Au nanospheres, which also did not adsorb any detectable serum protein in undiluted FBS.

For Au nanoparticles (NPs) of interest in biomedical imaging, the hydrodynamic diameter ( $D_h$ ) must be less than  $\sim 6$  nm for efficient renal clearance.<sup>1,2</sup> As these NPs are exposed to blood, the adsorption of even a single protein molecule on their surface, particularly the highly prevalent serum albumin ( $D_h \approx 7$  nm),<sup>3,4</sup> may increase the size too much for clearance. The adsorption of serum proteins on flat surfaces<sup>5–9</sup> and curved NPs<sup>10–14</sup> coated with nonionic, zwitterionic, or charged ligands depends in a complex manner on the surface orientation, charge, and hydrophobicity of the ligands.<sup>15–17</sup> Remarkably, precisely defined experiments to study renal clearance indicated that protein adsorption from 10% fetal bovine serum (FBS) was fully prevented with neutral [poly(ethylene glycol) (PEG)] or zwitterionic (cysteine) ligands but was high for charged ligands such as anionic dihydroliipoic acid (DHLA) and cationic cysteamine, respectively.<sup>1</sup> In numerous other studies, serum protein adsorption has been found to be relatively low on zwitterionic and nonionic surface coatings with zero net

charge.<sup>1,7,11,13,18</sup> For example, zwitterionic peptide ligands on flat Au surfaces synthesized from equal amounts of lysine ( $q = +1$ ) and glutamic acid ( $q = -1$ ) were shown to adsorb minimal amounts of the model serum proteins lysozyme and fibrinogen ( $<0.3$  ng of protein/cm<sup>2</sup>).<sup>8</sup> Similar low adsorption levels of these proteins were found for flat Au surfaces tailored with binary ligands with equal amounts of positive and negative charge.<sup>5,6</sup> The close spacings between the positive and negative charges on single zwitterionic ligands favor hydration and essentially zero protein adsorption on NPs, as measured by dynamic light scattering (DLS).<sup>11,19</sup>

For Au NPs coated with charged ligands, electrostatic interactions as well as charge–dipole interactions and specific interactions with hydrogen-bond donor and acceptor sites increase the adsorption relative to nonionic and zwitterionic ligands.<sup>1,5,20,21</sup> However, the roles of net charge and the topology of charge on the Au and protein surfaces on adsorption are not well-understood. For NPs coated with highly charged citrate, DHLA, or cysteamine ligands, adsorption of serum proteins has been found to increase  $D_h$  significantly, on the order of 10 nm.<sup>1,22,23</sup> For highly anionic citrate-capped Au NPs with zeta potentials ( $\zeta$ ) near  $-40$  mV,  $D_h$  increased from 30 to  $\sim 80$  nm upon incubation in undiluted human plasma.<sup>22</sup> Interestingly, very small ( $\sim 3$  nm), highly charged Au nanospheres coated with glutathione (GSH), which has two negative and one positive charge at neutral pH, were shown to be cleared efficiently through the kidneys.<sup>2</sup> While very low adsorption is typically measured with techniques such as gel electrophoresis,<sup>24,25</sup> surface plasmon resonance sensing,<sup>6,26</sup> and quartz crystal microbalance analysis,<sup>27</sup> these techniques do not have the sensitivity to measure the adsorption at the single protein molecule level, as can be done by DLS<sup>2,10,11,19</sup> or gel-filtration chromatography.<sup>1</sup>

Although charged monolayers on NPs composed of single ligands are not thought to resist protein adsorption,<sup>1,22,23,28</sup> relatively little is known about the behavior of NPs with binary and multicomponent mixed-charge monolayers. For binary zwitterionic mixtures with equal amounts of cationic and anionic ligands, adsorption is very low.<sup>5,6,8,26</sup> However, mixed monolayers of charged ligands, such as lysine/glutamic acid peptide monolayers on Au, bind significant amounts of proteins such as

Received: January 21, 2013

Published: April 8, 2013

fibrinogen and lysozyme ( $>50$  ng/cm<sup>2</sup>) when the lysine/glutamic acid ratio deviates from unity and the surface becomes charged.<sup>8</sup> However, Verma et al.<sup>10</sup> reported that Au nanospheres with ordered “stripes” of anionic mercaptoundecanesulfonate (MUS) and nonionic octanethiol (OT) adsorbed nearly zero serum protein upon incubation in 10% serum, as shown by a negligible change in  $D_h$  via DLS, despite a highly negative  $\zeta$  near  $-35$  mV. The inhibition of protein adsorption was attributed to the close proximity ( $\sim 5$  Å) of hydrophobic and hydrophilic groups on the nanosphere surface.<sup>10,29</sup> However, Yang and co-workers demonstrated that Au NPs and flat Au surfaces that do not adsorb protein in 10% human blood serum may adsorb significant amounts of protein in 100% serum.<sup>7,11</sup> Novel concepts are required to determine whether it is possible to form charged mixed monolayers that exhibit essentially zero protein adsorption even in undiluted serum.

In this work, we designed charged  $\sim 5$  nm Au nanospheres that adsorb essentially zero protein from undiluted FBS, as shown by a negligible increase in the  $D_h$  measured by DLS. The charged surfaces were tailored with binary ligand monolayers composed of two naturally occurring, relatively hydrophilic ligands, citrate ( $q = -3$ ) and either cationic lysine ( $q = +1$ ) or zwitterionic cysteine ( $q = 0$ ). The Au surface charge was tuned by place exchange of the citrate ligands with each amino acid, as characterized by  $\zeta$  and X-ray photoelectron spectroscopy (XPS). Relatively hydrophilic ligands were used to attempt to limit hydrophobic interactions that may increase adsorption.<sup>12,20,30</sup> For pure citrate or highly charged mixed-charge monolayers with high citrate levels,  $D_h$  increased by  $\sim 3$  nm or more as a result of protein adsorption. However, the change in  $D_h$  was negligible for lower citrate fractions, even for a moderate  $\zeta$  of  $-22$  mV in undiluted FBS. The zwitterionic tips of the lysine and cysteine ligands interact weakly with the protein and, furthermore, mitigate the interactions of the “buried” charges on the anchor groups at the Au surface. When the Au nanospheres were assembled into  $\sim 20$  nm nanoclusters of closely spaced primary NPs using an earlier methodology,<sup>31</sup> they exhibited intense near-IR (NIR) extinction that is of interest in biomedical applications, including photoacoustic imaging.<sup>32</sup> Upon biodegradation of PLA(1k)-*b*-PEG(10k)-*b*-PLA(1k) [PLA = poly(lactic acid)] on the surface of the nanoclusters, they dissociated into the original  $\sim 5$  nm constituent nanospheres, which totally resisted the adsorption of serum proteins.

To form binary mixed-charge monolayers on the surface of  $\sim 5$  nm Au nanospheres, citrate-capped nanospheres were first synthesized, and place-exchange reactions were conducted with either lysine or cysteine ligands [Figure 1a,b; see the Supporting Information (SI) for experimental procedures]. To determine the final ligand ratio on the nanosphere surface, excess ligands were removed by ultracentrifugation, and XPS was conducted on the dried nanosphere pellet (for details, see the SI). For lysine/citrate molar feed ratios from 4.5 and 9, place exchange led to final ligand ratios of 0.5 and 1.4 according to XPS (Table 1 and Figure S1 in the SI). The initial  $D_h$  value of  $4.3 \pm 0.8$  nm (Table 1) increased only slightly for both lysine/citrate ratios after place exchange (Table 1 and Figure 1c), as expected given the very small difference in the sizes of these two ligands relative to the diameter of the Au core. Inclusion of lysine at lysine/citrate ratios of 0.5 and 1.4 raised  $\zeta$  from the highly negative value of  $-58.4 \pm 5.3$  mV for pure citrate to  $-28.9 \pm 3.9$  and  $-16.1 \pm 2.9$  mV, respectively (Table 1). The ratios of these  $\zeta$  values to that for pure citrate were 49 and 28%, respectively, in good agreement with the ratios of 56 and 22% estimated from the number of

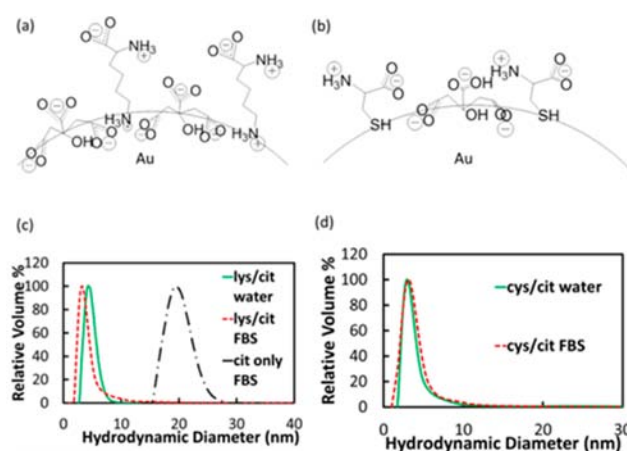


**Figure 1.** (a, b) Schematic illustrations of nanosphere surfaces coated with (a) citrate and lysine and (b) citrate and cysteine. (c, d) DLS distributions in water (green curve) and FBS (red curve) for nanospheres with (c) lysine/citrate = 1.4 and (d) cysteine/citrate = 1.6. The black curve in (c) is the DLS distribution for nanospheres capped only with citrate after FBS incubation.

**Table 1. Properties of Nanospheres Capped with Citrate or Binary Ligand Mixtures before and after Incubation in FBS**

ligand(s)	ligand ratio		$D_h$ (nm)	$\zeta$ (mV)	$D_h$ in FBS (nm)
	feed	XPS			
citrate	n/a	n/a	$4.3 \pm 0.8$	$-58.4 \pm 5.3$	$19.9 \pm 2.1$
Lys/citrate	4.5	0.5	$5.0 \pm 1.2$	$-28.9 \pm 3.9$	$7.7 \pm 3.8$
Lys/citrate	9	1.4	$4.6 \pm 1.1$	$-16.1 \pm 2.9$	$3.9 \pm 2.1$
Cys/citrate	0.3	1.0	$5.1 \pm 3.9$	$-28.8 \pm 3.2$	$8.8 \pm 5.8$
Cys/citrate	0.7	1.6	$3.4 \pm 2.5$	$-21.6 \pm 1.7$	$3.4 \pm 2.7$

charges on the ligands and the known ratios from XPS (Table S1 in the SI; see the SI for the calculation procedure and Tables S4–S7 for the reproducibilities of  $D_h$  and  $\zeta$ ).

For the place exchange of citrate with zwitterionic cysteine, smaller feed ratios were used than for lysine because of the stronger binding to Au by the cysteine thiol group relative to the lysine amino group. Again, the increase in  $D_h$  was negligible (Table 1 and Figure 1d). The final cysteine/citrate ligand ratios as determined by XPS were 1.0 and 1.6 for feed ratios of 0.3 and 0.7, respectively (Table 1 and Figure S1). The  $\zeta$  values were  $-28.8 \pm 3.2$  and  $-21.6 \pm 1.7$  mV, respectively, and the corresponding  $\zeta/\zeta_{\text{citrate}}$  ratios were 49 and 37%, in good agreement with the ratios of 49 and 39% calculated from the stoichiometries via XPS (Table S1).

The resistance of the charged mixed-monolayer nanospheres to serum protein adsorption was evaluated in 100% FBS. Here, even adsorption of a single 7 nm bovine serum albumin (BSA) or 14 nm immunoglobulin G molecule<sup>4</sup> would produce a substantial change in  $D_h$ . The adsorption of one BSA molecule would correspond to  $\sim 0.1$   $\mu\text{g}$  of BSA/cm<sup>2</sup> for a 5 nm Au nanosphere. For highly charged nanospheres with single ligands,  $D_h$  increased significantly, by 16 nm for citrate-capped nanospheres (Table 1 and Figure 1c) and 13 nm for GSH-capped nanospheres (Figure S2). In control experiments with DLS (see the SI), it was found that scattering from FBS solutions without added Au nanospheres was weak relative to the scattering by the Au nanospheres. For incubation in 100% FBS for lysine/citrate nanospheres at the lower ratio of 0.5,  $D_h$  increased only modestly (by 3 nm; Table 1). At the higher

lysine/citrate ratio of 1.4 ( $\zeta = -16.1$  mV), serum protein adsorption was completely inhibited, as the change in  $D_h$  was within the experimental error ( $<1$  nm; Table 1 and Figure 1c). Similar behavior was observed in the case of the cysteine/citrate mixed monolayers. For the lower cysteine/citrate ratio of 1.0,  $D_h$  increased by only 4 nm (Table 1). For a higher ratio of 1.6, however, protein adsorption was completely inhibited, as the change in  $D_h$  from  $3.4 \pm 2.5$  to  $3.4 \pm 2.7$  nm was within the experimental error (Table 1 and Figure 1d). Remarkably, not a single protein molecule was adsorbed, despite the substantial nanosphere surface charge ( $\zeta = -21.6 \pm 1.7$  mV). If protein molecules adsorb, they may cause aggregation of the Au nanospheres; however, our DLS distributions did not reveal any aggregates in the 100–1000 nm size range (Tables S8 and S9).

To support the DLS results, we measured nanosphere sedimentation in a centrifugal field. The Au yield by mass in the pellet was measured after centrifugation for 15 min at 10 000 rpm (see the SI). For Au nanospheres in deionized water, the yield was  $\sim 20\%$  in each case (see the SI). At the cysteine/citrate ratio of 1.6, a similar yield of 21% was observed in FBS, consistent with the lack of protein adsorption. However, for the ratio of 1.0, where  $D_h$  increased to 8.8 nm, the yield in the pellet increased to 39%, indicating that the centrifugation technique was also highly sensitive to protein adsorption. A similar trend was observed for lysine/citrate nanospheres (see the SI). Thus, the DLS and sedimentation techniques provided complementary evidence that the protein adsorption was negligible for the Au nanospheres coated with either cysteine/citrate or lysine/citrate ligands at the higher ratios. To our knowledge, these are the first examples of moderately charged gold nanospheres coated with binary mixed-charge ligands that completely prevent serum protein adsorption in undiluted serum. Furthermore, both ligands are naturally found in the body.

The significant levels of protein adsorption on citrate- and GSH-capped nanospheres can be partially attributed to overall electrostatic interactions between the negatively charged nanosphere surfaces and positively charged proteins as well as local charges and hydrogen-bonding sites on the protein surfaces. For example, Beurer et al.<sup>21</sup> found that protein adsorption on surfaces with a charge gradient from positively charged aminoundecanethiol to negatively charged mercaptoundecanoic acid was correlated with the overall electrostatic attraction, as negatively charged BSA and fibrinogen adsorbed mostly on the cationic quaternary ammonium section and positively charged lysozyme adsorbed mainly on the anionic carboxylates.<sup>21</sup> The most prevalent protein in serum, BSA, with an isoelectric point of 4.7,<sup>21</sup> is negatively charged at neutral pH, and thus, the overall electrostatic interaction with anionic Au surfaces is repulsive. However, interactions between the charged ligands and local charges and hydrogen-bonding sites on the protein surface must also be considered. For example, local attraction or salt bridges between cationic lysine residues on BSA and citrate ligands on Au nanospheres contribute to adsorption.<sup>28,33</sup> Thus, the serum protein adsorption observed on citrate- and GSH-capped nanospheres may be caused by overall electrostatic interactions with positively charged proteins as well as local electrostatic and hydrogen-bonding interactions with both positively and negatively charged proteins.

Our observation via DLS of essentially zero serum protein adsorption on a moderately charged binary monolayer was unexpected on the basis of previous studies with single-ligand monolayers<sup>1,28,33,34</sup> or mixed-charge monolayers with substantial

net charge.<sup>21,26</sup> For the lysine/citrate ratio of 1.4, the lack of protein adsorption suggests that the lysine screens the strong interactions of the trivalent citrate with the proteins, similar to the cysteine/citrate = 1.6 monolayers. The overall electrostatic interaction between the net negative charge of the binary monolayer and positively charged serum proteins is attractive. The difference in length of the citrate ligand versus either lysine or cysteine, however, may play an important role in resisting protein adsorption. For example, the zwitterionic tips of lysine or cysteine should interact weakly with protein surfaces because of the lack of net charge and strong hydration, as is known for other zwitterions.<sup>5,6,26</sup> Another important factor is that each of these amino acids is considerably longer than the citrate molecule (Figures 1a,b). The amino acids in the monolayers thus provide steric hindrance by increasing the distance between the three carboxylates on citrate and the protein surface. Thus, the local “buried” charges in the ligand monolayers should interact more weakly with the local charges and hydrogen-bonding sites on the protein surface. In addition, delocalization of the charge with the gold electrons for the two carboxylate anions on citrate and the protonated amine on lysine should further reduce the strength of the electrostatic interactions with the proteins.

Lysine, cysteine, and citrate are all highly hydrophilic, unlike hydrophobic ligands that facilitate adsorption of serum proteins by interacting with their hydrophobic segments.<sup>30</sup> For example, in the Hopp and Woods hydrophilicity index,<sup>35</sup> the hydrophilicity of lysine is 3.0, compared with 0.0 for glycine and  $-3.4$  for highly hydrophobic tryptophan. Cysteine is more hydrophobic than lysine (hydrophilicity of  $-1.0$ <sup>35</sup>) but hydrophilic enough to resist protein adsorption when combined with citrate in our mixed monolayers. In summary, the tunability of the ligand ratio and thus the surface charge for each of our mixed monolayers could be utilized to tailor the surfaces to resist protein adsorption even for moderate net charge.

Various techniques have been used to form nanoclusters with controlled properties from primary NPs.<sup>36</sup> The lysine/citrate = 1.4 nanospheres were assembled into nanoclusters upon solvent evaporation in the presence of a weakly adsorbing polymer, PLA-*b*-PEG-*b*-PLA, using a previously reported procedure<sup>31</sup> (see the SI). The nanoclusters with  $D_h = 21.7 \pm 4.3$  nm were composed of closely spaced primary Au nanospheres (Figure 2), which shifted

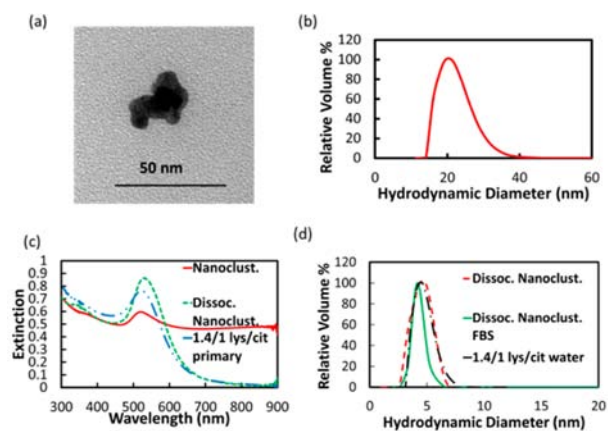


**Figure 2.** (a) TEM image, (b) DLS  $D_h$  distribution, and (c) UV-vis-NIR extinction spectrum (red) of lysine/citrate nanoclusters. In (c), spectra of dissociated nanoclusters and nanospheres are also shown. (d) DLS  $D_h$  distributions of dissociated nanoclusters, dissociated nanoclusters in FBS, and lysine/citrate nanospheres.

the extinction in the NIR from 650 to 900 nm. Incubation of the nanoclusters in pH 5 HCl for 24 h hydrolyzed the PLA(1k)-b-PEG(10k)-b-PLA(1k) on the surface, and the nanoclusters dissociated to Au nanospheres with the original nanosphere size, as shown by the UV-vis-NIR spectrum (Figure 2c) and the DLS size distribution (Figure 2d). The dissociated nanoclusters did not adsorb serum proteins, as  $D_h$  remained at only  $4.2 \pm 2.6$  nm (a desired size for kidney clearance) upon incubation in 100% FBS (Figure 2d).

In this robust colloidal assembly approach,<sup>31</sup> the size of the nanoclusters may be tuned as a function of the polymer and gold concentrations, the chemical structure of the surface ligands, and the extent of solvent evaporation. The biodegradable polymer adsorbs on the surface of the nanoclusters and quenches the size via an equilibrium mechanism.<sup>31c</sup> In the current study, we have shown for the first time that these clusters may be formed from Au particles with a surface charge that is large enough for nanocluster dissociation upon biodegradation of the polymer coating but small enough for full resistance to protein adsorption.

In conclusion, incubation of charged ~5 nm Au nanospheres with binary mixtures of natural and relatively hydrophilic ligands in undiluted serum protein does not increase the hydrodynamic diameter, indicating essentially zero protein adsorption. Moreover, the Au nanospheres can be assembled into NIR-active nanoclusters that biodegrade to primary Au nanospheres in vitro, again with essentially zero protein adsorption.

## ■ ASSOCIATED CONTENT

### Supporting Information

Experimental details and additional data. This material is available free of charge via the Internet at <http://pubs.acs.org>.

## ■ AUTHOR INFORMATION

### Corresponding Author

kpj@che.utexas.edu

### Notes

The authors declare no competing financial interest.

## ■ ACKNOWLEDGMENTS

K.P.J. and K.V.S. acknowledge support from NSF (CBET-0968038) and NIH (CA143663). K.P.J. and T.M.T. acknowledge support from the Welch Foundation (F-1319 and F-1696, respectively) and NSF (CBET-1247945). We thank a reviewer for suggesting the sedimentation experiments to support the DLS results for protein adsorption.

## ■ REFERENCES

- (1) Choi, H. S.; Liu, W.; Misra, P.; Tanaka, E.; Zimmer, J. P.; Ipe, B. I.; Bawendi, M. G.; Frangioni, J. V. *Nat. Biotechnol.* **2007**, *25*, 1165.
- (2) Zhou, C.; Long, M.; Qin, Y.; Sun, X.; Zheng, J. *Angew. Chem., Int. Ed.* **2011**, *50*, 3168.
- (3) Tirumalai, R. S.; Chan, K. C.; Prieto, D. A.; Issaq, H. J.; Conrads, T. P.; Veenstra, T. D. *Mol. Cell. Proteomics* **2003**, *2*, 1096.
- (4) Striemer, C. C.; Gaborski, T. R.; McGrath, J. L.; Fauchet, P. M. *Nature* **2007**, *445*, 749.
- (5) Holmlin, R. E.; Chen, X.; Chapman, R. G.; Takayama, S.; Whitesides, G. M. *Langmuir* **2001**, *17*, 2841.
- (6) Chen, S.; Yu, F.; Yu, Q.; He, Y.; Jiang, S. *Langmuir* **2006**, *22*, 8186.
- (7) Yang, W.; Xue, H.; Li, W.; Zhang, J.; Jiang, S. *Langmuir* **2009**, *25*, 11911.
- (8) Chen, S.; Cao, Z.; Jiang, S. *Biomaterials* **2009**, *30*, 5893.
- (9) Ostuni, E.; Chapman, R. G.; Holmlin, R. E.; Takayama, S.; Whitesides, G. M. *Langmuir* **2001**, *17*, 5605.

- (10) Verma, A.; Uzun, O.; Hu, Y.; Han, H.-S.; Watson, N.; Chen, S.; Irvine, D. J.; Stellacci, F. *Nat. Mater.* **2008**, *7*, 588.
- (11) Yang, W.; Zhang, L.; Wang, S.; White, A. D.; Jiang, S. *Biomaterials* **2009**, *30*, 5617.
- (12) Cedervall, T.; Lynch, I.; Lindman, S.; Berggård, T.; Thulin, E.; Nilsson, H.; Dawson, K. A.; Linse, S. *Proc. Natl. Acad. Sci. U.S.A.* **2007**, *104*, 2050.
- (13) Walkey, C. D.; Olsen, J. B.; Guo, H.; Emili, A.; Chan, W. C. W. *J. Am. Chem. Soc.* **2012**, *134*, 2139.
- (14) Larson, T. A.; Joshi, P. P.; Sokolov, K. *ACS Nano* **2012**, *6*, 9182.
- (15) Chen, S.; Li, L.; Zhao, C.; Zheng, J. *Polymer* **2010**, *51*, 5283.
- (16) Lundqvist, M.; Stigler, J.; Elia, G.; Lynch, I.; Cedervall, T.; Dawson, K. A. *Proc. Natl. Acad. Sci. U.S.A.* **2008**, *105*, 14265.
- (17) Markarucha, A. J.; Todorova, N.; Yarovsky, I. *Eur. Biophys. J.* **2011**, *40*, 103.
- (18) (a) Li, L.; Chen, S.; Zheng, J.; Ratner, B. D.; Jiang, S. *J. Phys. Chem. B* **2005**, *109*, 2934. (b) Liu, W.; Choi, H. S.; Zimmer, J. P.; Tanaka, E.; Frangioni, J. V.; Bawendi, M. J. *Am. Chem. Soc.* **2007**, *129*, 14530. (c) Ladd, J.; Zhang, Z.; Chen, S.; Hower, J. C.; Jiang, S. *Biomacromolecules* **2008**, *9*, 1357. (d) Estephan, Z. G.; Jaber, J. A.; Schlenoff, J. B. *Langmuir* **2010**, *26*, 16884.
- (19) Jia, G.; Cao, Z.; Xue, H.; Xu, Y.; Jiang, S. *Langmuir* **2009**, *25*, 3196.
- (20) Mahmoudi, M.; Lynch, I.; Eftehadi, M. R.; Monopoli, M. P.; Bombelli, F. B.; Laurent, S. *Chem. Rev.* **2011**, *111*, 5610.
- (21) Beurer, E.; Venkataraman, N. V.; Sommer, M.; Spencer, N. D. *Langmuir* **2012**, *28*, 3159.
- (22) Dobrovolskaia, M. A.; Patri, A. K.; Zheng, J.; Clogston, J. D.; Ayub, N.; Aggarwal, P.; Neun, B. W.; Hall, J. B.; McNeil, S. E. *Nanomedicine* **2009**, *5*, 106.
- (23) De Paoli Lacerda, S. H.; Park, J. J.; Meuse, C.; Pristiniski, D.; Becker, M. L.; Karim, A.; Douglas, J. F. *ACS Nano* **2010**, *4*, 365.
- (24) Yu, M.; Zhou, C.; Liu, J.; Hankins, J. D.; Zheng, J. *J. Am. Chem. Soc.* **2011**, *133*, 11014.
- (25) Liu, X.; Huang, H.; Jin, Q.; Ji, J. *Langmuir* **2011**, *27*, 5242.
- (26) Chen, S.; Zhen, J.; Li, L.; Jiang, S. *J. Am. Chem. Soc.* **2005**, *127*, 14473.
- (27) Kaufman, E. D.; Belyea, J.; Johnson, M. C.; Nicholson, Z. M.; Ricks, J. L.; Shah, P. K.; Bayless, M.; Pettersson, T.; Feldotó, Z.; Blomberg, E.; Claesson, P.; Franzen, S. *Langmuir* **2007**, *23*, 6053.
- (28) Brewer, S. H.; Glomm, W. R.; Johnson, M. C.; Knag, M. K.; Franzen, S. *Langmuir* **2005**, *21*, 9303.
- (29) Jackson, A. M.; Myerson, J. W.; Stellacci, F. *Nat. Mater.* **2004**, *3*, 330.
- (30) You, C.-C.; De, M.; Han, G.; Rotello, V. M. *J. Am. Chem. Soc.* **2005**, *127*, 12873.
- (31) (a) Tam, J. M.; Murthy, A. K.; Ingram, D. R.; Nguyen, R.; Sokolov, K. V.; Johnston, K. P. *Langmuir* **2010**, *26*, 8988. (b) Tam, J. M.; Tam, J. O.; Murthy, A.; Ingram, D. R.; Ma, L. L.; Travis, K.; Johnston, K. P.; Sokolov, K. V. *ACS Nano* **2010**, *4*, 2178. (c) Murthy, A. K.; Stover, R. J.; Borwankar, A. U.; Nie, G. D.; Gourisankar, S.; Truskett, T. M.; Sokolov, K. V.; Johnston, K. P. *ACS Nano* **2013**, *7*, 239.
- (32) Yoon, S. J.; Mallidi, S.; Tam, J. M.; Tam, J. O.; Murthy, A.; Johnston, K. P.; Sokolov, K. V.; Emelianov, S. Y. *Opt. Lett.* **2010**, *35*, 3751.
- (33) Dominguez-Medina, S.; McDonough, S.; Swanglap, P.; Landes, C. F.; Link, S. *Langmuir* **2012**, *28*, 9131.
- (34) Casals, E.; Pfaller, T.; Duschl, A.; Oostingh, G. J.; Püntes, V. *ACS Nano* **2010**, *4*, 3623.
- (35) Hopp, T. P.; Woods, W. R. *Proc. Natl. Acad. Sci. U.S.A.* **1981**, *78*, 3824.
- (36) (a) Zhuang, J.; Wu, H.; Yang, Y.; Cao, Y. C. *Angew. Chem., Int. Ed.* **2008**, *47*, 2208. (b) Ma, L. L.; Feldman, M. D.; Tam, J. M.; Paranjape, A. S.; Cheruki, K. K.; Larson, T. A.; Tam, J. O.; Ingram, D. R.; Paramita, V.; Villard, J. W.; Jenkins, J. T.; Wang, T.; Clarke, G. D.; Asmis, R.; Sokolov, K.; Chandrasekar, B.; Milner, T. E.; Johnston, K. P. *ACS Nano* **2009**, *3*, 2686. (c) Xia, Y. S.; Nguyen, T. D.; Yang, M.; Lee, B.; Santos, A.; Podsiadlo, P.; Tang, Z. Y.; Glotzer, S. C.; Kotov, N. A. *Nanotechnol.* **2011**, *6*, 580. (d) Lu, Z.; Yin, Y. *Chem. Soc. Rev.* **2012**, *41*, 6874.